A Ratiometric Expressible FRET Sensor for Phosphoinositides Displays a Signal Change in Highly Dynamic Membrane Structures in Fibroblasts†

Gregor Cicchetti,* Melinda Biernacki,‡ Jessica Farquharson, and Philip G. Allen

Hematology Division and Department of Medicine, Brigham and Women's Hospital and Harvard Medical School, 221 Longwood Avenue, Boston, Massachusetts 02115

Received August 19, 2003; Revised Manuscript Received November 26, 2003

ABSTRACT: Phosphoinositides are important signal transduction intermediates in cell growth, survival, and motility. We have invented a fluorescence sensor for polyphosphorylated phosphoinositides based on a peptide derived from the *Listeria* protein ActA that undergoes a random coil to helix transition upon lipid binding. The sensor, termed CAY, is a fusion protein of cyan and yellow fluorescent proteins flanking the peptide at its N- and C-termini, respectively. CAY displays fluorescence resonance energy transfer *in vitro* in the absence of phosphorylated phosphoinositides, and this energy transfer is lost upon interaction with these phospholipids. These results demonstrate that a short peptide undergoing a coil to helix transition can be sufficient for the engineering of a FRET-based biosensor. CAY is predominantly localized to the cytoplasm in fibroblasts expressing the sensor but shows loss of fluorescence resonance energy transfer in regions of active actin dynamics such as ruffles that have previously been demonstrated to contain high levels of phosphoinositides.

Phosphoinositides are important elements of multiple cellular pathways, including vesicle transport and fusion, cell motility, calcium release from internal stores, cell survival, and oncogenesis (*1*−*3*). Phosphatidylinositol can be phosphorylated at positions 3−5 to generate multiple isoforms of phosphorylated phosphoinositides. A large number of enzymes regulate the generation and degradation of these lipids. Phosphoinositide binding domains such as PH-domains,[1] FYVE domains, or Phox homology domains bind individual phosphoinositide molecules with high affinity and selectivity but do not undergo structural transformations upon binding their lipid targets (*4*). Fluorescent derivatives of these molecules have been successfully used to qualitatively assess changes in phosphoinositide distribution and, by implication, concentration, in response to cell activation (*5*−*10*).

Many proteins regulating the actin cytoskeleton in cells interact with and are regulated by phosphorylated phosphoinositides. These proteins either directly bind to actin or are part of signaling cascades controlling actin polymerization. They include actin severing proteins such as gelsolin (*11*) and cofilin (*12*), actin capping proteins such as gelsolin and CapZ (*13*), actin cross-linking proteins such as α-actinin (*14*) and filamin (*15*), the G-actin binding protein profilin (*16*), the focal adhesion proteins vinculin (*17*) and talin (*18*), signaling proteins such as N-WASp (*19*), CDC42 (*20*), and Rac (*21*), and the bacterial surface protein ActA (*22*, *23*). None of these proteins contain PH-domains that bind specifically to the hydrophilic headgroups of particular phosphoinositide isoforms (*4*), and virtually all of them contain relatively short, positively charged peptide sequences responsible for phosphoinositide binding. When tested *in vitro*, these proteins bind phosphorylated phosphoinositides with micromolar affinity and low isoform specificity. In contrast to PH-domains, phosphoinositide binding leads to conformational changes in talin (*18*), gelsolin (*24*), profilin (*25*), vinculin (*17*), N-WASp (*26*), and ActA (*22*). Little is known about which areas of cell membranes allow interaction of these proteins with phosphoinositides in intact cells. This is in contrast to localization studies of PH-domains fused with fluorescent proteins that indicate that a sufficient concentration of target lipids exists in cells to explain the localization of the full-length protein (*5*, *6*).

Invention of ratiometric sensors to address localization and concentration of target molecules in cells has allowed investigators to overcome the problems of two-dimensional measurements of three-dimensional objects and differential segregation of probes. This approach originated with small molecule sensors for various ions and has been extended in recent years using fluorescence resonance energy transfer (*27*, *28*). FRET occurs between a donor fluorophore and an acceptor molecule with the emission spectrum of the donor overlapping with the absorption spectrum of the acceptor.

† Supported in part by NIH RO1 Grant GM 57256 and NIH Training Grant HL07680.

* To whom correspondence should be addressed: Hematology Division and Department of Medicine, Brigham and Women's Hospital and Harvard Medical School, 221 Longwood Ave., Boston, MA 02115. Telephone: (617) 278-0339. Fax: (617) 734-2248. E-mail: gcicchetti@rics.bwh.harvard.edu.

‡ Present address: Department of Medical Oncology, Dana-Farber Cancer Institute, 44 Binney St., Boston, MA 02115.

[1] Abbreviations: PI(3,4,5)P_3, phosphatidylinositol 3,4,5-trisphosphate; PI(3,4)P_2, phosphatidylinositol 3,4-bisphosphate; PI(4,5)P_2, phosphatidylinositol 4,5-bisphosphate; PI(4)P, phosphatidylinositol 4-monophosphate; PI(3)P, phosphatidylinositol 3-monophosphate; PI, phosphatidylinositol; PC, phosphatidylcholine; PH-domain, pleckstrin homology domain; FRET, fluorescence resonance energy transfer; G-actin, globular actin; N-WASp, neuronal Wiskott-Aldrich-Symptom protein; GFP, green fluorescent protein; CFP, cyan variant of GFP; YFP, yellow variant of GFP; MEF, mouse embryonic fibroblast; PDGF, platelet-derived growth factor; PlC-δ, phospholipase C-δ; PI 3-kinase, phosphoinositide 3-kinase.

10.1021/bi035480w CCC: $27.50
Published on Web 01/31/2004

The acceptor molecule can be either a fluorophore or a chromophore. FRET-based ratiometric sensors are often expressible protein sensors that undergo a conformation change upon ligand binding and are flanked by two different fluorophores capable of FRET. The intensity of FRET changes in the presence or absence of the respective ligand and allows for the detection of the concentration of a particular ligand and its cellular localization *in vivo* (*29*, *30*). FRET occurs between spectral variants of the green fluorescent protein, making them ideally suited fluorophores for protein sensors. Expressible FRET-based protein sensors have been used to detect changes in calcium ions, cAMP, cGMP, and particular protein kinase activities (*31*−*36*).

To determine whether cells contain membrane domains capable of supporting lipid binding by the short, cationic phosphoinositide binding sequences identified in actin binding proteins, we used a peptide sequence from the surface protein ActA from *Listeria monocytogenes* as a phosphoinositide binding unit in a ratiometric FRET sensor. This sequence has been shown to undergo a random coil to α-helical structural transition upon phosphoinositide binding and is predicted to form an amphipathic helix in the presence of lipid bilayers containing these lipids (*22*). The efficiency of FRET is highly sensitive to the distance between the fluorophores, and an α-helix of a length similar to that of ActA is sufficiently rigid to maintain fluorophore separation (*37*). We find that there is significant change in FRET of a fusion protein containing the ActA peptide tagged N-terminally by CFP and C-terminally by YFP in the presence of phosphoinositides *in vitro* and in live cells.

EXPERIMENTAL PROCEDURES

Cell Culture, Microinjection, and Transfection. Swiss 3T3 fibroblast cells were obtained from ATCC and cultivated in DMEM (Gibco Invitrogen, Carlsbad, CA) containing 10% FBS. Mouse embryonic fibroblasts expressing the tetracycline-controlled transactivator tTA (MEF Tet-Off) were obtained from BD Biosciences Clontech (Palo Alto, CA) and cultivated in DMEM containing 0.5 mg/mL G418. Cells were microinjected with DNA using a MO-150 micromanipulator and an IM200 pressure injector (Narishige, Tokyo, Japan). Two hours after injection, the medium was changed for imaging into an optical clear medium and the cells were analyzed. OptiMEM (Gibco) or HAM'S F-12K (BIOfluids, Rockville, MD) supplemented with 0.5 mM $CaCl_2$ with or without 10% FBS was used as an optical clear medium. Both media were supplemented with 10 mM HEPES (pH 7.4) as well as penicillin (100 units/mL), streptomycin (100 μg/mL), and amphotericin B (0.25 μg/mL). All supplements were from Gibco except when stated otherwise. MEF Tet-Off cells were transfected in 10 cm dishes with pTreCAY using Superfect (Qiagen, Hilden, Germany) according to the manufacturer's recommendations. The superfect-DNA mix was removed after 1 h, and after 48 h, the cells were split one to four into DMEM containing 0.5 mg/mL G418, 0.3 mg/mL hygromycin, and 10 μg/mL doxycycline (Clontech). After 1 week, clones were picked, further subcloned, and tested for CAY expression upon removal of doxycycline. MEF-CAY cells were cultivated in DMEM containing 0.5 mg/mL G418, 0.1 mg/mL hygromycin, and 10 μg/mL doxycycline. Doxycycline was removed to induce CAY expression. For PDGF stimulation experiments, CAY cells were serum starved overnight in DMEM and transferred to HAM's F-12K medium 25 min prior to the experiment. When wortmannin or LY294002 (Calbiochem, San Diego, CA) was used, it was added 30 min prior to cell stimulation.

Cloning of GFP-ActA184−*235, CY, CAY, Citrine-Containing CAY, and FLAG- or GFP-Tagged PH-Domains.* A vector encoding amino acids 185−235 of ActA (pActA55) (*22*) was cleaved with *Eco*RI and *Hin*dIII, and the insert was subcloned into pEGFP-C1 (Clontech) digested with the same restriction enzymes, resulting in pGFP-ActA185−235. pEYFP (Clontech) was cleaved with *Age*I and *Xba*I, and the insert was subcloned into pECFP-C1 (Clontech) cleaved with *Xma*I and *Xba*I, resulting in pECFP-YFP. This vector was used to express CY, a CFP-YFP fusion protein lacking the phosphoinositide-binding site. CY contains a 23-amino acid linker between the CFP and the YFP unit with the sequence SGLRSRAQASNSAVDGTAGPVAT. To purify CY in COS7 cells, a His tag was introduced by mixing two oligonucleotides encoding the His tag (CTAGCCGCCACCATGGGATCGCATCACCATCACCATCACACA and CCGGTGTGTGATGGTGATGGTGATGCGATCCCATGTGGCGG) at a molar ratio of 1/1, heating them to 90 °C for 1 min, and ligating them into the *Age*I and *Nhe*I sites of pECFP-YFP, resulting in pECFP-YFPHis. A PCR to amplify DNA encoding ActA184−235 was performed using pActA55 as a template and the following primers: CTCGAGCTCAAGCTTCG and GCGGTACCGTCCGAAGCATTTACCTCTTC. The PCR product was cleaved with *Kpn*I and inserted into pECFP-YFP, resulting in pCAY. pCAY was cleaved with *Eco*47III and *Bcl*I or with *Nhe*I and *Not*I, and the inserts were subcloned into pQE100 (Qiagen) digested with *Sma*I and *Bgl*II and pTre2hyg (Clontech) digested with *Nhe*I and *Not*I, resulting in pCAY100 and pTreCAY, respectively. For the generation of citrine-containing CAY, pRESB containing the DNA for citrine (a kind gift from O. Pertz) was cleaved with *Bsr*I, *Bse*RI, and *Hae*II, the 580 bp fragment was isolated and ligated with the 200 bp *Bsr*I, *Not*I, and the 2675 bp *Not*I, *Bse*RI fragments of pEYFP (Clontech). The resulting vector was cleaved with *Bsr*GI and *Bse*RI, and the 678 bp fragment was ligated with the 270 bp *Bsr*GI, *Bse*RI and the 4675 bp *Bsr*GI, *Bsr*GI fragments of pCAY. Vectors encoding GFP-tagged PH-domains of PlC-δ and Akt were based on pEGFP-C1 and were cleaved with *Age*I and *Bsr*GI. Oligonucleotides encoding a FLAG tag (CCGGTATGGATTACAAGGATGACGACGATAAGCT and GTACAGCTTATCGTCGTCATCCTTGTAATCCATA) were mixed at a molar ratio of 1/1, heated to 90 °C for 1 min, and ligated into these vectors, resulting in pPH-PlC-δ-FLAG and pPH-AKT-FLAG. pCAY as well as pECFP-YFPHis, pPH-PlC-δ-FLAG, and pPH-AKT-FLAG was sequenced to confirm the proper nucleotide sequence and orientation.

Purification of CAY and CY. Cultures (1 L) of *Escherichia coli* Xl1 Blue cells harboring pCAY100 were induced for 1 h at 25 °C with 0.1 mM IPTG at an OD of 0.5. Since we were not able to purify CY from *E. coli*, COS7 cells in 15 cm dishes were transiently transfected with pECFP-YFPHis. Cells (*E. coli* or COS) were harvested, sonicated in PBS supplemented with 0.5% Triton X-100 and protease inhibitors (Sigma, St. Louis, MO), and centrifuged at 5000*g* for 15 min. Supernatants were loaded on a 5 mL Ni−NTA column (Qiagen) equilibrated with buffer A [50 mM sodium

phosphate and 300 mM NaCl (pH 8)]. The column was washed with 50 mM sodium phosphate, 500 mM NaCl, and 10% glycerol (pH 7), and proteins eluted in a gradient of 0 to 250 mM imidazole in buffer A. Fractions containing a high concentration of CAY were pooled, desalted into buffer B [50 mM Tris-HCl and 50 mM NaCl (pH 8)], and applied to a 5 mL MonoQ column (Pharmacia). Proteins were eluted using a gradient of 0 to 50% 50 mM Tris-HCl and 1 M NaCl (pH 7) in buffer B, and fractions containing high concentrations of CAY were analyzed by fluorescence spectroscopy and SDS−PAGE for purity and integrity and subsequently pooled, snap-frozen, and stored at −80 °C.

Preparation of Lipids and Spectroscopic Analysis of CAY. D$_3$-Phosphoinositides were obtained from Matreya Inc. (State College, PA); all other lipids were from either Sigma or Avanti (Alabaster, AL). Lipids were dissolved in water mixed at the appropriate ratio and sonicated at 40 W using a W 185 F sonicater (Heat System, Ultrasonics Inc., Plainview, NY) until the suspension was optically clear. CAY lipid interactions were analyzed at 37 °C in PBS (pH 7.2) supplemented with 0.1 mg/mL GST using a Perkin-Elmer LS-50 or a Photon Technology Inc. QM4 fluorescence spectrophotometer. The excitation wavelength was set to 435 nm (±5 nm); emission scans from 450 to 600 nm were recorded, and the ratio of emission intensities of 476 nm to 525 nm was determined. Apparent K_d values were determined using the dose−response logistic algorithm within the Kaleidagraph program (Synergy Software, Reading, PA). For trypsin digestion, 1 mL of a solution with 1 mg/mL CAY was incubated with 2 units of trypsin for 60 min. Aliquots were taken at 0, 10, 20, and 30 min and diluted 1/30-fold, and the emission spectra of the sample were recorded immediately.

Microscopy of CAY-Expressing Cells and Data Analysis. Cells transiently or permanently expressing CAY, citrine-containing CAY, or a GFP- or FLAG-tagged PH-domain of Akt were analyzed using an inverted epifluorescence microscope (Diaphot 300, Nikon) equipped with shutter, excitation, and emission filter wheels and a mercury lamp. Cells were plated into 35 mm dishes with a glass coverslip bottom (Matek Corp., Ashland, MA) which was gridded for CAY−PH-domain co-injection experiments and kept at 37 °C using a cell heater with a controller (models PDMI2 and TC202, Medical System Corp., Greenvale, NY). Images were taken with a cooled CCD camera (CCD-1300-Y, Roper Scientific, Trenton, NJ). The CFP portion of CAY or CY was excited using a 440 nm (±10 nm) band-pass filter; a dichroic filter with a cutoff at 455 nm was used, and CFP emission was recorded using a 480 nm (±15 nm) band-pass filter. A 535 nm (±15 nm) filter was used to record YFP emission. Cells were imaged using either a 40× Nikon plan or a 40× Nikon plan fluor oil objective except when stated otherwise. All optical filters used for analysis of FRET were obtained from Omega Opticals Inc. (Brattleboro, VT). Data were analyzed and processed using Isee (Inovision Software), NIH-image, and Adobe Photoshop. Ratio images were obtained by pixel by pixel division of the 480 nm image over the 535 nm image and scaled by 1000. For photobleach experiments, the YFP part of CAY was bleached using a 546 nm (±10 nm) band-pass filter (Chroma Technology Inc., Brattleboro, VT). A 40 min exposure resulted in approximately 30% bleaching of YFP. For FLAG staining, cells were fixed with 3.7% formaldehyde for 10 min followed by complete bleaching of YFP. Cells were then immunostained using a mouse monoclonal anti-FLAG antibody (clone M2 SIGMA) and a rabbit rhodamine-labeled secondary antibody (Jackson Immuno Research Laboratories, West Grove, PA). The variance was defined as the sum of the absolute values of the difference between the mean pixel intensity and each pixel. For analysis of the mean ratio intensity and the variance of ratio intensities, only whole cells with a maximum fluorescence intensity of 200 units or more and a minimal area of 100 μm^2 were used.

RESULTS

Construction of the Phosphoinositide Specific FRET Sensor. The bacterial surface protein ActA of the facultative pathogen *L. monocytogenes* contains a region in its N-terminus that binds polyphosphorylated phosphoinositides and induces a random coil to α-helix transition in the molecule (*22*). We designed the fusion protein CAY that consists of CFP, ActA amino acids 184−235, and YFP (Figure 1A). The construct was cloned into mammalian (pEGFP and pTRE, Clontech) as well as bacterial (pQE 100, Qiagen) expression vectors. The His-tagged bacterially expressed protein was purified by Ni−NTA affinity chromatography and anion exchange chromatography, and homogeneity was assessed by gel electrophoresis and Coomassie staining.

In Vitro Properties of CAY. Purified CAY exhibits efficient energy transfer in the absence of lipids with a substantial yellow emission upon excitation of CFP at 435 nm, the optimal wavelength for CFP excitation, with the YFP emission peak at 525 nm being roughly in equal intensity to the CFP emission peak at 476 nm (Figure 1A). In the presence of 10 μM PI(4,5)P$_2$, PI(3,4)P$_2$, or PI(3,4,5)P$_3$, CAY displays a significant reduction in the intensity of the yellow emission with a corresponding increase in the intensity of the cyan emission, consistent with a structural change diminishing the level of FRET (Figure 1A,B). PI, PC, or phosphatidylserine did not change the FRET signal of CAY (Figure 1B). Phosphoinositides were presented as pure sonicated lipids or as small unilamellar vesicles (SUVs) in a background of PC containing either 10 or 0.2 mol % phosphoinositides. In either case, the apparent K_d value for interaction of CAY with PI(3,4,5)P$_3$ was 0.6 μM, those for PI(3,4)P$_2$ and PI(4,5)P$_2$ were 1 μM, and those for PI(3)P and PI(4)P were 1.7 μM (Figure 2 and data not shown). Small unilamellar vesicles (SUVs) containing PI or PC vesicles alone were tested up to 50 and 200 μM, respectively, and did not induce any FRET change in CAY (Figure 2 and data not shown). The maximal ratio difference between the lipid-bound form and the nonbound form of CAY was ∼2-fold for PI(3,4,5)P$_3$ and 1.8- and 1.6-fold for bisphosphorylated and monophosphorylated phosphoinositides respectively (Figure 2 and data not shown). Addition of 0.1% Triton X-100 to CAY in the presence of phosphorylated phosphoinositides restored the baseline FRET signal of CAY (Figure 1 of the Supporting Information). Addition of 300 μM D-myoinositol 1,4,5-trisphosphate, the headgroup of PI(4,5)-P$_2$, had no effect on the FRET signal of CAY, nor did it affect its ability to interact with PI(4,5)P$_2$ (Figure 1C). Likewise, addition of D-myoinositol 1,3,4,5-tetrakisphosphate did not alter the spectra of CAY or its ability to interact

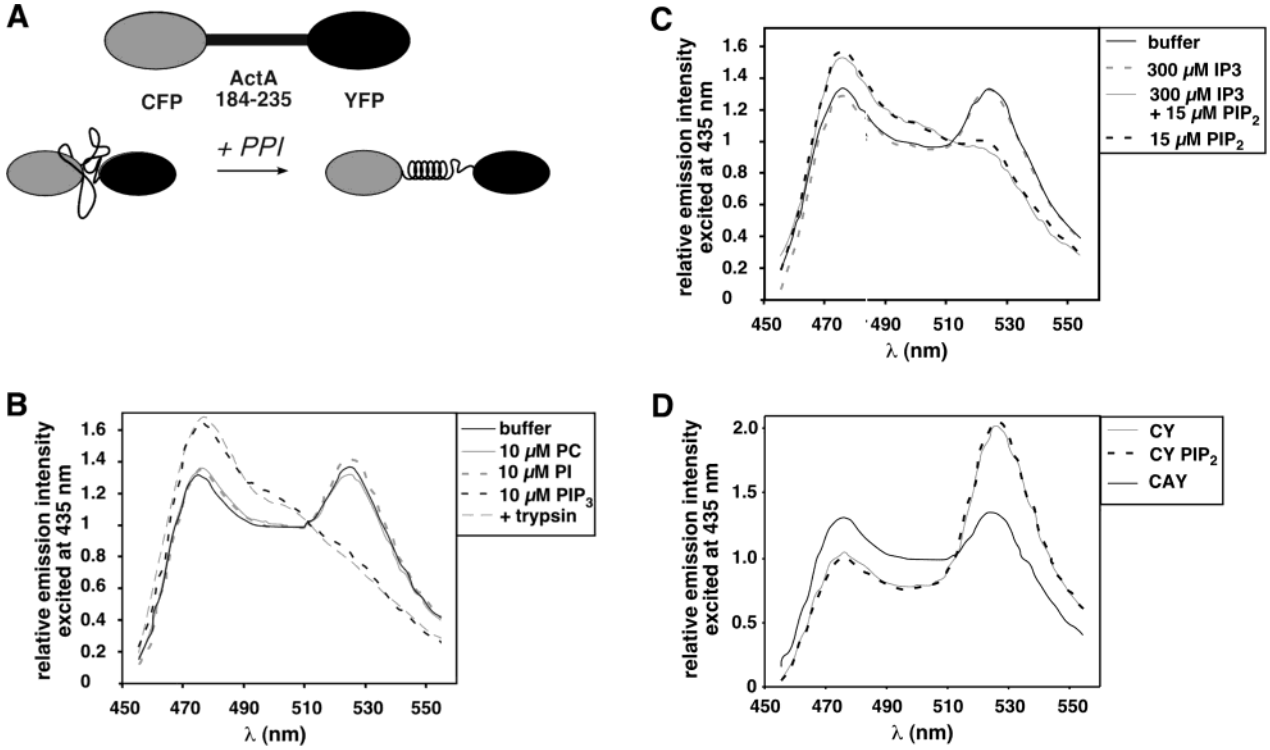

FIGURE 1: CAY displays a loss in FRET signal intensity in the presence of polyphosphorylated phosphoinositides. A schematic depiction of CAY and its conformational status in the absence and presence of phosphoinositides is depicted in panel A. The phosphoinositide binding site of ActA (amino acids 184−235) is flanked by the cyan-emitting (CFP) and yellow-emitting (YFP) mutants of green fluorescent protein. In the presence of phosphoinositides, the random coil converts to a helix, altering the distance between the fluorophores. (B and C) Fluorescent spectra of CAY. CAY was excited at 435 nm (±5 nm), and an emission spectrum was recorded as described in Experimental Procedures. In panel B, CAY displayed a characteristic two-peak spectrum in buffer (—) which did not change significantly in the presence of either 10 μM phosphatidylinositol (PI) or phosphatidylcholine (PC). The emission peak at 525 nm was lost in the presence of 10 μM phosphatidylinositol 3,4,5-trisphosphate (PIP_3) or after treatment with trypsin (− − −). For trypsin treatment, a 1 mg/mL solution of CAY was incubated with 2 units of trypsin for 50 min and an aliquot was taken out and measured immediately. As displayed in panel C, addition of 300 μM inositol 1,4,5-trisphosphate (PIP_3) did not alter the spectrum of CAY (—), and further addition of 15 μM phosphatidylinositol 4,5-bisphosphate (PIP_2) resulted in a CAY spectrum that was indistinguishable from that of CAY with 15 μM PIP_2 alone (- - -). In panel D, CY (thin line) displayed more FRET than CAY (thick line) in buffer alone, but its spectrum did not change in the presence of 20 μM $PI(4,5)P_2$ (dashed line). All spectra were normalized to 1 at the isosbestic point of 512 nm.

with $PI(3,4,5)P_3$ (Figure 1 of the Supporting Information). These data indicate that the acyl−glycerol backbone of phosphoinositides is essential for CAY−lipid interaction, consistent with data obtained with full-length ActA (*22*). To determine the maximal loss of FRET and to control for inappropriate excitation of YFP at 435 nm, CAY was proteolyzed with trypsin (2 units/mg of CAY). Proteolysis induced an increase in the intensity of the cyan emission at 488 nm and a decrease in the intensity of the yellow emission at 535 nm. After digestion for 50 min, the relative cyan and yellow emissions were similar to that observed in the presence of saturating concentrations of polyphosphorylated phosphoinositides, indicating that lipid binding to CAY results in a complete loss of FRET (Figure 1B). CY, a fusion of the cyan and yellow fluorescent proteins separated by a 23-amino acid linker (see Experimental Procedures), exhibited a high degree of FRET upon excitation of CFP at 435 nm with the YFP emission peak being double the intensity of the CFP emission peak (Figure 1D). However, addition of 20 μM $PI(4,5)P_2$ had no effect on the spectra of CY (Figure 1D). In summary, these results suggest that CAY is a sensitive, ratiometric FRET sensor for phosphorylated phosphoinositides with affinity and selectivity similar to those reported for numerous proteins regulating the actin cytoskeleton.

In Vivo Properties of CAY. To determine whether CAY was a useful sensor for phosphoinositides in cells, DNA encoding CAY (pCAY) was microinjected into Swiss 3T3 fibroblasts and protein expression was monitored 2−4 h following microinjection. CAY was located predominately in the cytoplasm and the nucleus as indicated by the cyan emission image (Figure 3A, 480 nm) and the yellow emission image (Figure 3A, 535 nm). This was in agreement with data obtained with the expression of a fusion protein consisting of GFP fused to the phosphoinositide binding site of ActA (amino acids 184−235 of ActA) in Swiss 3T3 fibroblasts. This protein was approximately 2-fold enriched in dynamic membrane areas when compared against a volume marker (Figure 3 of the Supporting Information).

CAY was excited with 440 nm (±10 nm) light, and emission images were recorded using 480 (±15 nm) and 535 nm (±15 nm) band-pass filters. After background subtraction, the ratio of emission intensities at 480 nm to 535 nm was calculated and scaled by 1000. The ratio image revealed a highly uniform value for the ratio of emission at 480 nm to 535 nm throughout the cell. Consistent with the benefits of ratiometric measurements, the ratio was independent of the cell thickness, while the emission intensity for each fluorophore was not (Figure 3A, top two panels). Once the YFP component of the fusion protein had been bleached, the cyan

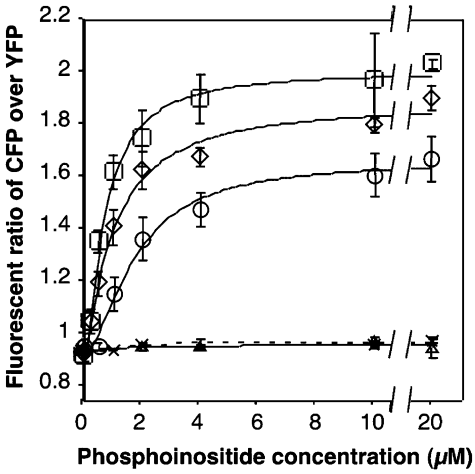

FIGURE 2: CAY interacts specifically with polyphosphorylated phosphoinositides with a micromolar affinity *in vitro*. CAY was incubated with SUVs consisting of phosphatidylcholine and phosphoinositides at a molar ratio of 9:1. The ratio of 475 nm to 535 nm emission intensity of CAY, which is inversely proportional to the FRET signal, is plotted against increasing concentrations of phospholipids. The CAY FRET signal decreases significantly with increasing concentrations of phosphorylated phosphatidylinositols, but not with phosphatidylcholine (△) or phosphatidylinositol (×). CAY had a higher affinity for phosphatidylinositol 3,4,5-trisphosphate (□) than for either phosphatidylinositol 4,5-bisphosphate (◇) or phosphatidylinositol 4-monophosphate (○) under these conditions. All measurements were performed at 37 °C.

emission intensity at 480 nm increased as the yellow emission intensity at 535 nm decreased (Figure 2 of the Supporting Information). This result strongly suggests that CAY not bound to its ligand exhibits FRET *in vivo*. Since CAY interacts with a variety of phosphoinositides *in vitro* with a micromolar K_d and phosphoinositide concentrations in the cytoplasmic membrane are believed to be in the range of 10 μM (*38*), it is conceivable that CAY interacts with phosphoinositides throughout the cytoplasmic membrane. This should result in a higher ratio of CAY in very thin sections of the cell since the ratio of soluble to membrane-associated CAY can be assumed to significantly different from that in thick parts of the cell. However, as displayed in Figures 3 and 4, the ratio of CAY is highly uniform across the cell, even when comparing very thin cell sections with areas around the nucleus that display a more than 10-fold increase in fluorescence intensity. This result strongly suggests that CAY does not interact with the bulk of membranes in the cell.

Previous studies using PH-domains specific for particular phosphoinositides suggest that ruffles are enriched in both $PI(4,5)P_2$ and $PI(3,4,5)P_3$ (*7*, *10*). Interestingly, highly active membrane protrusions such as dorsal ruffles showed the largest changes in FRET emission by CAY (Figures 3A and 4). In contrast, when CY was expressed in Swiss 3T3 cells, it showed little or no change in the ratio of cyan over yellow emission under similar conditions (Figure 3B). This demonstrates that the ratio change observed with CAY is dependent on the presence of the phosphoinositide binding peptide in the fusion protein.

To provide an experimental cell system useful for screening phosphoinositide concentrations in the cell, we generated a mouse embryonic fibroblast cell line with CAY under the control of the TET promoter (TetOff, Clontech). The MEF−CAY cells expressed high levels of CAY after removal of tetracycline. Serum-starved MEF−CAY cells ruffled extensively within 5 min of stimulation by 12 ng/mL PDGF. As in cells transiently expressing CAY, the level of FRET was greatly diminished in these ruffles (Figure 4A). We did not observe a significant loss of FRET in lateral extensions until these extensions lifted off the substrate (Figure 4B). This observation correlates with data obtained using GFP-tagged PH-domains of Akt or PlC-δ (Figure 9 of the Supporting Information and data not shown). To quantify the degree of FRET loss in ruffles, pixel intensity profiles through dorsal ruffles were obtained. As expected, a relative increase in the intensity of the cyan emission signal over that of the yellow emission signal as well as a significant loss of FRET in ruffles was observed in CAY-expressing cells, but not in cells expressing CY (Figures 3C,D and 4C, left panels). The ratio of the emission intensities of cyan to yellow in these areas was typically 1.3−1.7 times higher than in the rest of the cell (Figures 3C and 4C, right panels) which is very much in agreement with the relative change in CAY emission ratios measured *in vitro* in the presence and absence of phosphoinositides. This demonstrates that CAY displays changes in FRET *in vivo*, the level of FRET decreasing in regions of active cytoskeletal and membrane dynamics.

The spectral properties of the yellow variant of GFP can be altered by ionic or pH changes in the environment (*39*). To exclude any contributions from such effects to the observed FRET change of CAY in membrane ruffles, we created a similar fusion protein containing a pH- and halide-insensitive variant of YFP, citrine (*40*). Upon injection into serum-starved MEFs and stimulation with PDGF, FRET loss was observed in ruffles indistinguishable to cells expressing CAY (Figure 4 of the Supporting Information).

PI 3-kinase inhibitors, wortmannin or LY294002, drastically reduced the extent of ruffle formation and loss of CAY FRET in MEF−CAY cells stimulated with PDGF. Likewise, cells not stimulated with PDGF displayed no ruffling activity or CAY FRET change (Figure 5 of the Supporting Information). To further examine whether CAY was responding to $PI(4,5)P_2$ or $PI(3,4,5)P_3$ in ruffling cells, competition experiments with PH-domains specific for $PI(4,5)P_2$ and $PI(3,4,5)P_3$ were performed. The PH-domain of the protein kinase Akt interacts specifically with $PI(3,4)P_2$ and $PI(3,4,5)P_3$, whereas the PH-domain of PlC-δ binds $PI(4,5)P_2$ (*41*). Mixtures of DNA encoding CAY and either FLAG-tagged PH-domains of Akt, or PlC-δ, were injected into Swiss 3T3 fibroblasts. Expression of the PH-domain of Akt almost completely abolished FRET changes in ruffles (Figure 5A), whereas cells coexpressing CAY with the PH-domain of PlC-δ displayed a FRET signal change in ruffles similar to that in cells expressing CAY alone (Figure 5B). This suggests that the PH-domain of Akt competes with CAY binding *in vivo*. The immunofluorescence with anti-FLAG antibodies confirmed expression of the PH-domains in the cells in Figure 5. Quantitative imaging of the immunostaining of the FLAG motif indicated that there was an approximately 2-fold higher concentration of the PH-domain of PlC-δ than of the Akt domain. Since the cell expressing the PH-domain of Akt was 2.35 times the size of the cell expressing the PH-domain of PlC, total expression levels of the two proteins were comparable.

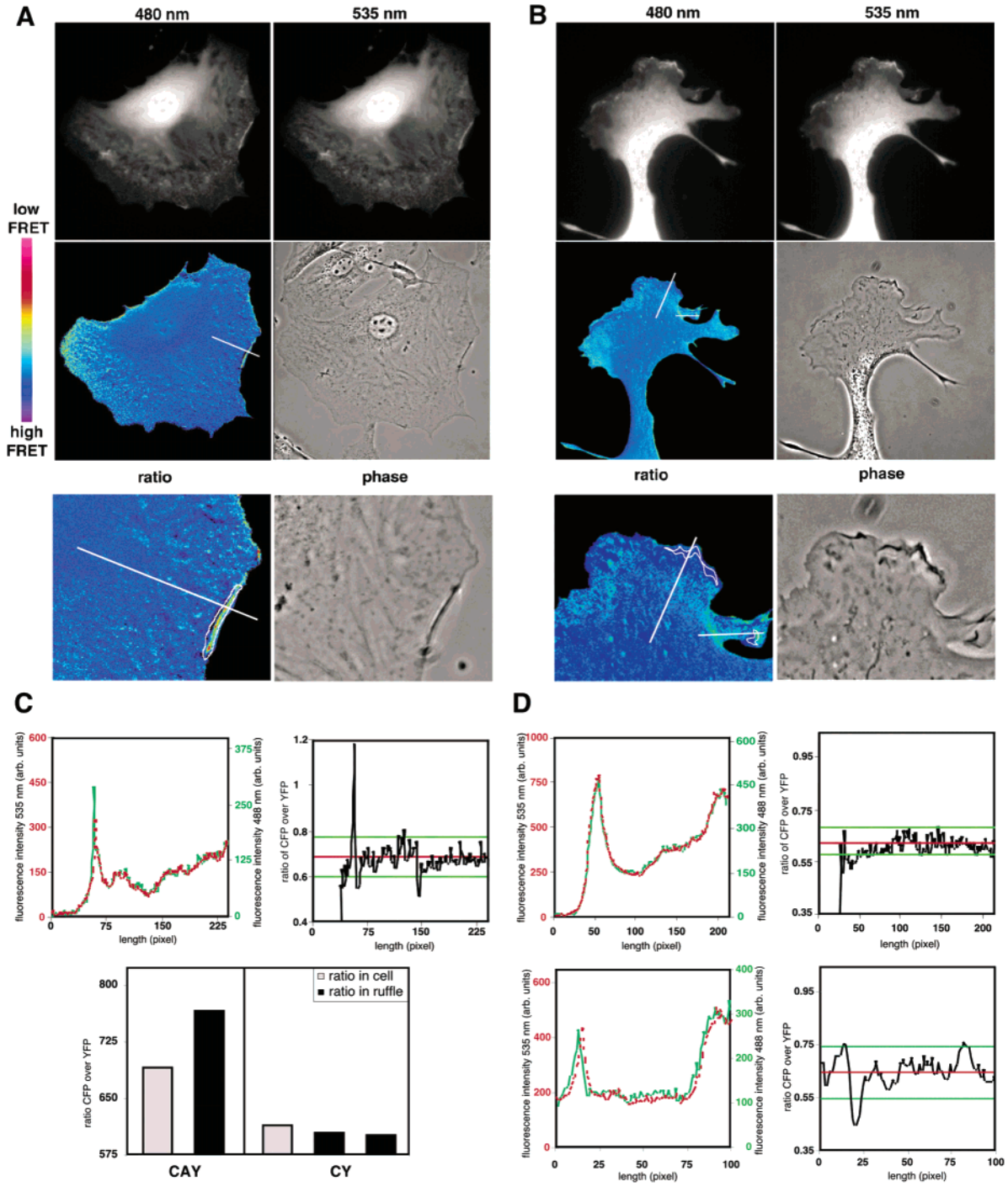

FIGURE 3: CAY displays a loss of FRET in ruffles *in vivo*. Swiss 3T3 fibroblasts were microinjected with expression vectors encoding GFP fusion proteins and imaged 3 h after injection, and ratio images were obtained as described in Experimental Procedures. In panel A, the cyan (480 nm) and yellow (535 nm) emission images, as well as the ratio and phase images of a cell injected with CAY, are illustrated. FRET loss is depicted with warmer colors. It is predominantly observed in a ruffle, and the ratio and phase image of an inset magnifying the ruffle is displayed. In panel B, a loss of FRET in dynamic membrane ruffles was not observed in cells expressing cyan and yellow fluorescent proteins with a 23-amino acid linker lacking the lipid binding domain. The parts of panel B are arranged in a manner identical to that in panel A. The color table indicates ratio values from 400 (high FRET) to 1200 (low FRET) in panel A and from 350 (high FRET) to 1050 (low FRET) in panel B. (C) A pixel intensity profile of the white line in the ratio image of panel A is displayed in the top right subpanel. The *x*-axis of all pixel intensity plots represents the lines from the cell edge (pixel 0) to the inner part of the cell (high pixel number). The red line indicates the mean ratio of a box of 100 pixels × 100 pixels surrounding the cellular area of the line; the green lines reflect the mean ± two standard deviations. The top left subpanel displays pixel intensity profiles of the cyan emission image (green) and the yellow emission image (red). The scales of the *y*-axis of the upper left subpanel correspond to fluorescence intensities of both images that were normalized to a region in the cell that displayed no ruffle activity. The bottom subpanel displays analysis of regions that were drawn around whole ruffles analyzed with the intensity profiles based on the fluorescence images. The regions are outlined in the bottom left subpanels of panels A and B. The mean intensity of the ratio image (ratio in ruffle) was determined and compared to that of a nearby region identical in size (ratio in cell). (D) Pixel intensity profiles as in panel C. The top two subpanels correspond to the long line and the lower two subpanels to the short line.

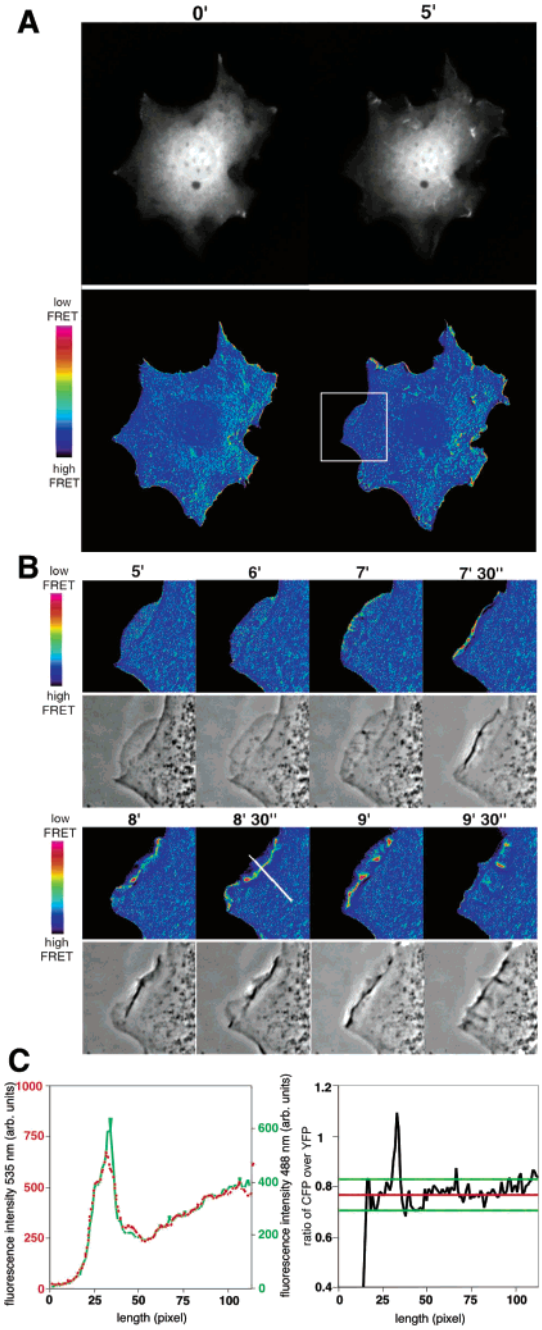

FIGURE 4: PDGF induces ruffles with loss of FRET of CAY. Mouse embryonic fibroblasts stably expressing CAY were serum starved overnight and stimulated with PDGF, and ratio images were obtained as described in Experimental Procedures. Panel A illustrates the CFP fluorescence (top panel) and ratio (bottom panel) of a cell before stimulation with PDGF and 5 min after stimulation. Panel B displays an inset from panel A which illustrates that transient localization of CAY FRET loss is restricted to dorsally protruding ruffles. The top subpanel displays the ratio and the bottom subpanel the phase images. The color table indicates ratio values from 500 (high FRET) to 1500 (low FRET). In panel C, pixel intensity profiles of the white line in panel B are displayed. The *x*-axis represents the line from the cell edge (pixel 0) to the inner part of the cell (high pixel number). The right subpanel shows the pixel intensity profile of the ratio image. The red line indicates the mean ratio of a box of 100 pixels × 100 pixels surrounding the cellular area of the line; the green lines reflect the mean ± two standard deviations. The left subpanel displays pixel intensity profiles of the cyan emission image (green) and the yellow emission image (red). The scales of the fluorescence intensities of the left subpanel were normalized to a region in the cell which displayed no ruffle activity.

Taken together, these results demonstrate that CAY is a reporter for polyphosphorylated phosphoinositides in cells and recognizes its targets in ruffles, regions of active actin dynamics and shape change. CAY does not undergo a conformational change in ruffles when coexpressed with the PH-domain of Akt, suggesting $PI(3,4,5)P_3$ and $PI(3,4)P_2$ are necessary but may not be sufficient for CAY FRET change *in vivo*.

The ability to detect a change in a sensor rapidly and efficiently is the key to effective screening. While our CAY ratiometric sensor has significant advantages over current technology because of the phosphoinositide-induced changes in emission spectra, the limited distribution of the signal change in the cell may make it difficult to detect changes in phosphoinositide concentration from the average changes in the emission ratio. Because of the low selectivity of CAY *in vitro* and the spatially constrained signal change of CAY in the cell, the current version of CAY might be useful in specialized cases as a screening sensor. However, because of its short sequence and low level of secondary structure, the phosphoinositide binding peptide of ActA could provide an excellent basis for mutagenesis studies by altering its affinity and selectivity. We wanted to test whether the observed FRET change in CAY in ruffles upon stimulation would be large enough to be detected in an automated system. Cells were stimulated with PDGF, and low-magnification ratiometric images of cell clusters were generated (Figure 6A). While the mean value of the ratio of 475 nm to 525 nm did not change significantly over time upon PDGF stimulation (Figure 6 of the Supporting Information), the variance increased drastically over time (Figure 6B,C). No increase in the variance was observed in cells expressing CY or cells expressing CAY treated with the PI 3-kinase inhibitor LY294002 (panels B and C of Figure 6; Figure 6 of the Supporting Information), consistent with d_3-phosphoinositide generation being necessary to diminish the level of FRET in ruffles. Not every cell in a population reacts to growth factors to the same degree, and accordingly, the change in variance was striking in most, but not all, single cells (Figure 7 of the Supporting Information). However, it was significant in all cell populations that were analyzed (Figure 6C; Figure 7 of the Supporting Information). Consistent with the much lower affinity of our CAY sensor for phosphoinositide compared with the PH-domain of AKT, the time course of variance change was slower than that of PIP_3-dependent AKT phosphorylation in these cells. However, peak AKT phosphorylation is consistent with the maximal increase in variation that we observed (Figure 8 of the Supporting Information) and with observations made by Auger *et al.* analyzing $PI(3,4,5)_3$ and $PI(3,4)P_2$ production upon PDGF stimulation in smooth muscle cells (*42*). These data suggest that MEF−CAY cells could be useful in screening for alteration in phosphoinositide concentration or organization necessary for the regulation of actin binding proteins in the cell.

DISCUSSION

Phosphoinositides are important regulators of cell migration (*43*), cell transformation (*44*), and cell survival (*45*). Identifying the sites of generation and concentration of these lipids provides a greater insight into how these lipids act. We have shown that a 50-amino acid peptide that undergoes

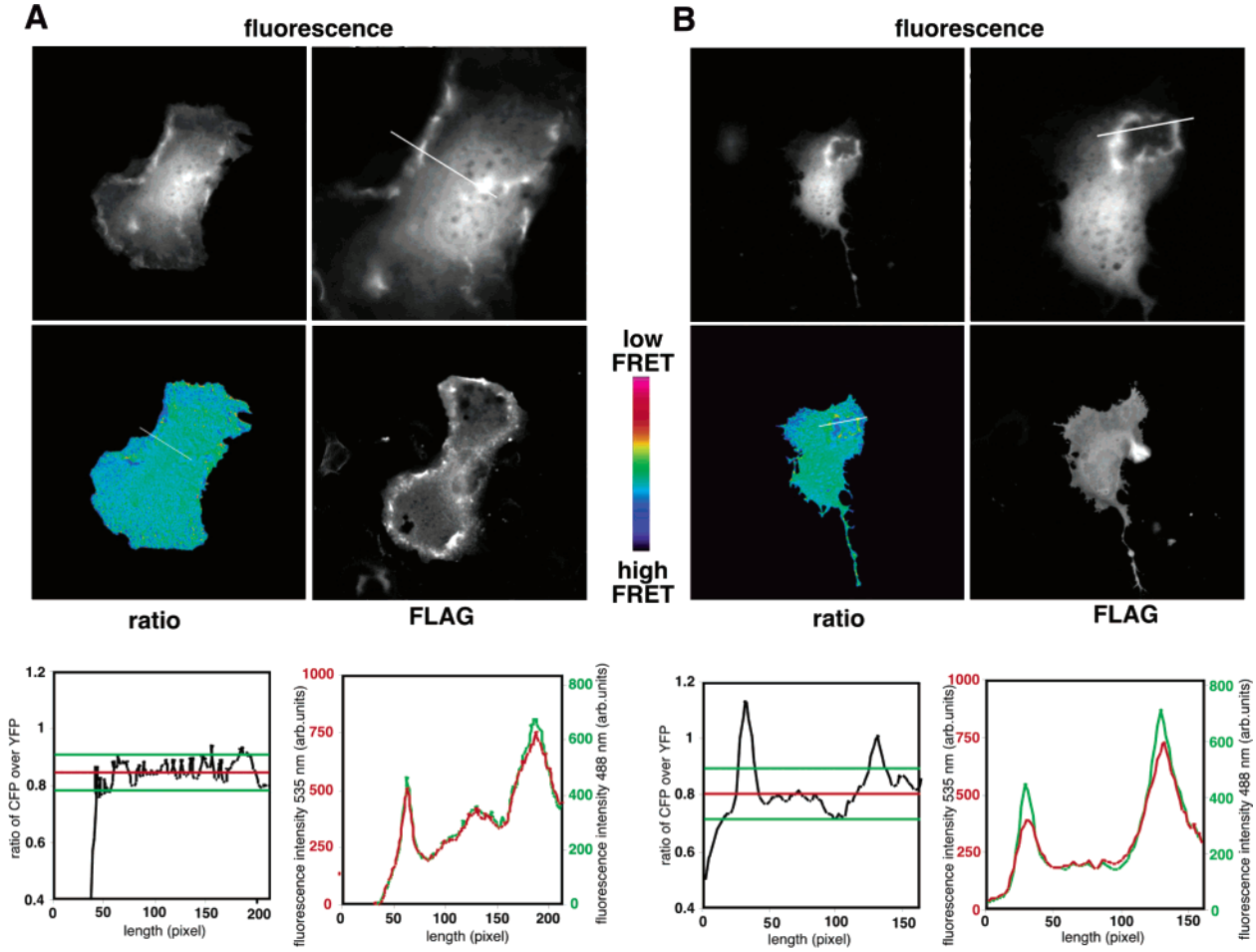

FIGURE 5: PH-domain of Akt but not of PlC-δ supresses FRET loss of CAY in ruffles. Ratio images were obtained as described in Experimental Procedures. Coexpression of CAY with the PH-domain of Akt, binding specifically $PI(3,4)P_2$ and $PI(3,4,5)P_3$ (A), but not the PH-domain of PlC-δ, which binds $PI(4,5)P_2$ (B), inhibited FRET loss in CAY. Both PH-domains were N-terminally FLAG-tagged. The emission ratio of CAY and the phase images are compared to the localization of the PH-domains with the anti-FLAG antibody. Note that cells were fixed approximately 7 min after the live images were taken. The color table indicates ratio values from 470 (high FRET) to 1410 (low FRET). Pixel intensity profiles of the white lines in top two panels are displayed in the bottom subpanel. The *x*-axis represents the line from the cell edge (pixel 0) to the inner part of the cell (high pixel number). The second and fourth bottom subpanels from the left show the pixel intensity profiles of the ratio images. The red line indicates the mean ratio of a box of 100 pixels $\times$ 100 pixels surrounding the cellular area of the line; the green lines reflect the mean $\pm$ two standard deviations. The first and third lower subpanels from the left display pixel intensity profiles of the cyan emission image (green) and the yellow emission image (red). The scales of the *y*-axis correspond to the fluorescence intensities of both images that were normalized to a region that displayed no ruffle activity.

a random coil to helix transformation upon binding phosphoinositides can be used as a ratiometric sensor when flanked by fluorescent protein domains capable of undergoing fluorescence resonance energy transfer (FRET). The CAY fusion of the ActA peptide flanked by cyan and yellow fluorescent proteins displays a spectral shift upon lipid binding, allowing the detection of phosphoinositides by changes in the spectral emission, not intensity, of the sensor. In contrast, existing single-color lipid-binding domains, such as fusions of GFP with the appropriate PH-domain, are completely dependent on the change in their intracellular distribution in reporting alterations in phosphoinositide metabolism.

Peptide sequences that undergo a random coil to α-helix transition upon target binding provide a structural change that, coupled with the appropriate fluorophores, can be detected through changes in the emission spectra due to resonance energy transfer. CAY's characteristic loss of FRET upon lipid-induced helix formation is consistent with studies of other peptides similar in length. A linker of 37 amino acids that is predicted to form a random coil allows significant energy transfer between cyan and yellow fluorescent proteins (*46*), while an α-helical linker of only 25 amino acids drastically reduces the efficiency of energy transfer (*37*). For CAY, the loss of FRET is consistent with a previous report of lipid-induced helix formation in the core peptide (*22*), and the degree of FRET loss is consistent with other sensors for Ca^{2+} (*31*), cGMP (*34*), or phosphotyrosine (*36*) that depend on conformational changes of linked ligand binding and sensor motifs. A fusion of a 19-amino acid phosphoinositide binding peptide derived from gelsolin, which is also known to undergo a coil to helix transition upon lipid binding (*47*), when flanked by CFP and YFP did not provide a large change in the FRET signal.[2] This is possibly due to its short sequence of only 10 amino acids that undergoes the conformational change and becomes α-helical.

[2] Unpublished observation.

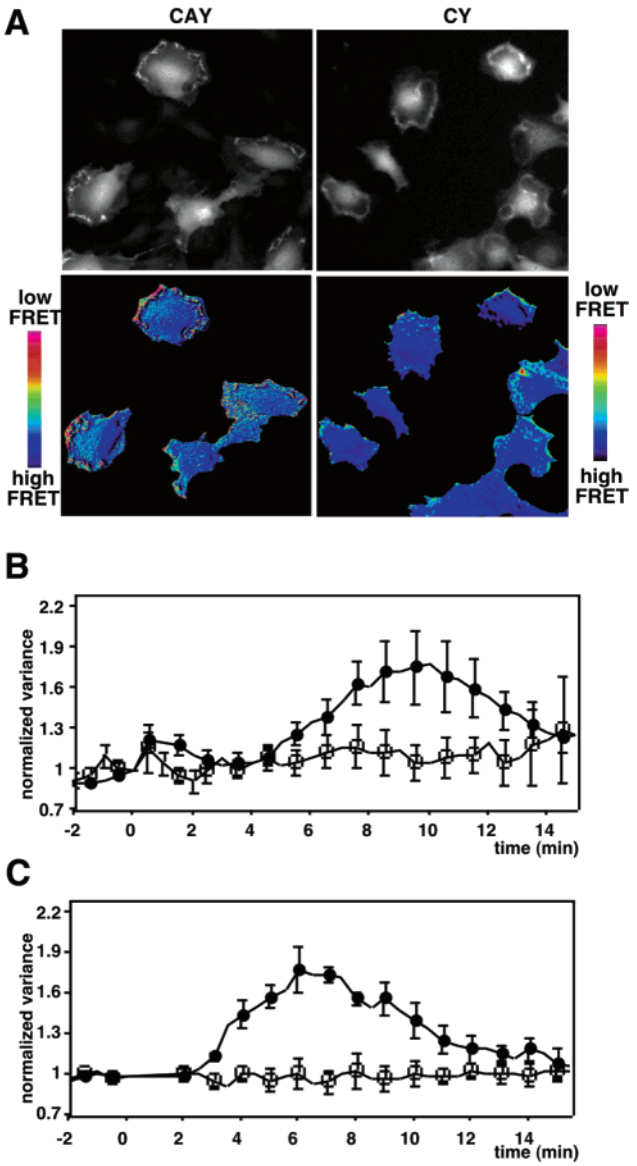

FIGURE 6: Stimulation of MEFs expressing CAY with PDGF increases the variance of ratio images. Mouse embryonic fibroblasts expressing CAY or CY were serum starved overnight and stimulated with 12 ng/mL PDGF, and ratio images were obtained as described in Experimental Procedures. In panel A, the top subpanel depicts the CFP fluorescence and the bottom subpanel the ratio 10 min after induction. The color table indicates ratio values from 500 or 350 (high FRET) to 1500 or 1050 (low FRET) for CAY- or CY-expressing cells, respectively. Only the cells depicted in the bottom subpanel were used for further analysis in panels B and C. The means of the variance of the pixel intensity of the ratio of all single cells of one experiment (panel B) or of groups of cells of at least three independent experiments (panel C) were plotted over time: (●) cells expressing CAY and (□) cells expressing CY. Variance values were normalized to 1 at the time of the stimulation; PDGF was added at time 0. Error bars represent standard errors of the mean.

When expressed in cells, CAY's spectral change likely reports the location of high concentrations of phosphoinositides. CAY spectral changes suggest that the highest concentrations of phosphoinositides are found in spatially constrained regions of active cytoskeletal and membrane dynamics such as ruffles. These regions have previously been suggested to be high in both $PI(4,5)P_2$ and $PI(3,4,5)P_3$ (*7*, *48*, *49*), though some data also suggest that these claims may be, at least in part, an artifact of membrane folding (*50*). In contrast, the spectral change in CAY is insensitive to the apparent concentration of the sensor. We do not detect significant global increases in the level of CAY FRET over the entire cell upon PDGF stimulation as would be expected from studies using the PH-domain of Akt which binds $PI(3,4)P_2$ as well as $PI(3,4,5)P_3$ with high affinity (*5*). This could be either due to its relatively low affinity for phosphoinositides or due to a spatial restriction of CAY−phosphoinositide interactions to distinct areas of the cytoplasmic membrane. However, even when imaged at a low magnification, the FRET change of CAY was robust enough to reproducibly cause a large change of variance in the ratio image, suggesting that CAY-expressing cells are potentially useful in an automated high-throughput screening setting for modulators of phosphoinositides. Probes that change only their spatial localization, such as fluorescently labeled PH-domains, have been used to analyze changes in phosphoinositide metabolism in cells (*5*, *7*, *10*, *48*, *49*). However, the automated interpretation of such spatial changes is complicated. Furthermore, many of the existing probes having a high affinity for specific phospholipid isoforms have substantial cytotoxicity, and no stable cell lines expressing these proteins have been reported.

PI 3-kinase inhibition by wortmannin or LY294002 inhibited the spectral change of CAY, as did coexpression of a PH-domain that binds $PI(3,4,5)P_3$ and $PI(3,4)P_2$, but not a PH-domain that binds $PI(4,5)P_2$. There is an apparent contradiction, however, between the *in vivo* data suggesting that the sensor detects high concentrations of $PI(3,4)P_2$ or $PI(3,4,5)P_3$ and the minor selectivity differences we observe *in vitro*. This could be due to many factors, including regulatory connections between PI 3-kinase and membrane ruffle formation (*51*), modulatory roles of PI 3-kinase products on $PI(4,5)P_2$ levels (*52*), or modulation of selectivity *in vivo* by the local membrane structure or environment. Many proteins involved in regulating the actin cytoskeleton such as gelsolin, vinculin, profilin, cofilin, WASp-family proteins, and α-actinin interact with phosphoinositides and do not contain a PH-domain. When tested *in vitro*, all of these proteins display affinities for phosphorylated phosphoinositides in the micromolar range and little specificity for distinct phosphoinositide isoforms (*12*, *14*, *17*, *26*, *53*). However, unlike proteins containing PH-domains, most of these proteins are not localized at nondynamic areas of the cytoplasmic membrane even though the concentration for D-4 phosphorylated phosphoinositides in the plasma membrane has been shown to be in the range of tens of micromolar (*38*). This raises the possibilities that these proteins have a higher isoform specificity *in vivo* than *in vitro* and that only selected areas of the membrane support lipid binding. Phosphoinositide binding peptides such as the one used in CAY, or a peptide derived from the actin binding protein gelsolin that also undergoes a coil to helix transition upon lipid binding (*47*), do not interact with the headgroups of phosphoinositides alone (Figure 1 and ref *11*), and one component of the recognition event may be the hydrophobic environment of the bilayer. Membrane curvature, local charge density, and the nature of other membrane lipids are likely to influence the binding specificity as well as the binding affinity of CAY. Consistent with this hypothesis, phosphoinositide binding of CAY, gelsolin, and CapZ is interrupted

by the detergent Triton X-100 (Figure 1 of the Supporting Information and refs *13* and *53*). Moreover, the presence of other lipids alters the phosphoinositide binding affinity for the actin binding protein gelsolin (*53*). In the cell, the abundance of other phosphoinositide binding proteins competing for binding sites may also influence binding specificity.

Some PH-domains have been shown to have high phosphoinositide binding specificity and affinity *in vitro* and have been used as probes to visualize the phosphoinositide distribution *in vivo*. However, recently elucidated experimental data suggest that PH-domains recognize phosphoinositides in cellular membranes only in the context of additional factors (*54*). Even though a variety of experimental data suggest that PI(4,5)P_2 is present in almost all membranes of the cell (*55*, *56*), PH-domains predominantly detect PI(4,5)P_2 in the plasma membrane (*9*). Very recently, a FRET sensor utilizing the PH-domain of GRP1, which binds PI(3,4,5)P_3 and PI(3,4)P_2 was reported (*57*). This biosensor is tethered to the membrane, and binding of the PH-domain to the target lipid causes a rearrangement of the CFP and YFP components of the sensor. While this is the first specific ratiometric sensor for PI(3,4,5)P_3 production, it has a small dynamic range when targeted to the plasma membrane. Also, this PH-domain binds its lipid target with nanomolar affinity, making it difficult to sense high local lipid concentrations. Consistent with our suggestion that PIP_3 is necessary for inducing the conformation change in our CAY sensor, the time course of PIP_3 production at the plasma membrane detected using the sensor developed by Sato *et al*. is nearly identical to that illustrated in Figure 6.

Detection of the significantly more abundant lipid PI(4,5)P_2 has been accomplished using intermolecular FRET. In the work of van der Wal *et al*. (*8*), single cyan or yellow fluorescent protein−PH−PlC-δ fusion constructs were cotransfected into cells, and the change in intermolecular FRET was detected upon stimulation of lipid hydrolysis. Violin *et al*. (*58*), simplified this approach by constructing a cyan and yellow PlC−PH fusion. In this case, there was no change in intramolecular FRET with lipid binding, but intermolecular FRET changed with the changing PIP_2 concentration. While this two-color, intermolecular sensor prevented common experimental difficulties derived from different concentrations of the donor and acceptor, the change in the signal was quite small. The advantage of these approached is that the respective sensor specifically detects single molecular species in contrast to CAY and similar peptides which interact *in vitro* with multiple phosphoinositides. The CAY-like peptides, however, are more suitable for detecting higher local concentrations of these lipids. Taken together, information about phosphoinositide distribution and concentration obtained with peptides such as CAY might supplement data obtained with PH-domains.

Using a peptide motif undergoing a conformational change upon target binding has a major advantage in that it allows for the development of a ratiometric biosensor. Binding phosphoinositides with a relatively low affinity likely prevents the detection of low phosphoinositide concentrations in the cell, but it is also less likely to interfere with the high-affinity interactions occurring in signaling cascades. The CAY peptide has the further advantage of no apparent cellular toxicity and provides a basis for future mutagenesis studies for developing peptides with altered affinity and selectivity.

ACKNOWLEDGMENT

We thank Rose Asrican for technical assistance. We also thank Walther Mothes, Marc Lemmon, and Tobias Meyer for providing the GFP-tagged PH-domains of PlC-δ and Akt and Olivier Pertz and Roger Y. Tsien for providing citrine. We are grateful to Chris Carpenter, Alan Lader, Luis Vidali, Hervé Falet, and Tom Stossel for fruitful discussions.

SUPPORTING INFORMATION AVAILABLE

Interaction of CAY with inositol 1,3,4,5-tetrakisphosphates and Triton X-100, bleaching of CAY, single-color expression of GFP-ActA184−235, MEFs expressing citrine, the lack of FRET change in unstimulated or wortmannin-treated CAY cells, and FRET variance of single-CAY expressing cells and of different cell populations. This material is available free of charge via the Internet at http://pubs.acs.org.

REFERENCES

1. Cantrell, D. A. (2001) *J. Cell Sci. 114*, 1439−1445.
2. Nishizuka, Y. (1984) *Science 225*, 1365−1370.
3. Toker, A., and Cantley, L. C. (1997) *Nature 387*, 673−676.
4. Itoh, T., and Takenawa, T. (2002) *Cell. Signalling 14*, 733−743.
5. Gray, A., Van Der Kaay, J., and Downes, C. P. (1999) *Biochem. J. 344* (Part 3), 929−936.
6. Stauffer, T. P., Ahn, S., and Meyer, T. (1998) *Curr. Biol. 8*, 343−346.
7. Tall, E. G., Spector, I., Pentyala, S. N., Bitter, I., and Rebecchi, M. J. (2000) *Curr. Biol. 10*, 743−746.
8. van der Wal, J., Habets, R., Varnai, P., Balla, T., and Jalink, K. (2001) *J. Biol. Chem. 276*, 15337−15344.
9. Varnai, P., and Balla, T. (1998) *J. Cell Biol. 143*, 501−510.
10. Varnai, P., Rother, K. I., and Balla, T. (1999) *J. Biol. Chem. 274*, 10983−10989.
11. Janmey, P. A., and Stossel, T. P. (1987) *Nature 325*, 362−364.
12. Yonezawa, N., Nishida, E., Iida, K., Yahara, I., and Sakai, H. (1990) *J. Biol. Chem. 265*, 8382−8386.
13. Heiss, S. G., and Cooper, J. A. (1991) *Biochemistry 30*, 8753−8758.
14. Fukami, K., Furuhashi, K., Inagaki, M., Endo, T., Hatano, S., and Takenawa, T. (1992) *Nature 359*, 150−152.
15. Furuhashi, K., Inagaki, M., Hatano, S., Fukami, K., and Takenawa, T. (1992) *Biochem. Biophys. Res. Commun. 184*, 1261−1265.
16. Lassing, I., and Lindberg, U. (1985) *Nature 314*, 472−474.
17. Gilmore, A. P., and Burridge, K. (1996) *Nature 381*, 531−535.
18. Martel, V., Racaud-Sultan, C., Dupe, S., Marie, C., Paulhe, F., Galmiche, A., Block, M. R., and Albiges-Rizo, C. (2001) *J. Biol. Chem. 276*, 21217−21227.
19. Rohatgi, R., Ma, L., Miki, H., Lopez, M., Kirchhausen, T., Takenawa, T., and Kirschner, M. W. (1999) *Cell 97*, 221−231.
20. Zheng, Y., Glaven, J. A., Wu, W. J., and Cerione, R. A. (1996) *J. Biol. Chem. 271*, 23815−23819.
21. Missy, K., Van Poucke, V., Raynal, P., Viala, C., Mauco, G., Plantavid, M., Chap, H., and Payrastre, B. (1998) *J. Biol. Chem. 273*, 30279−30286.
22. Cicchetti, G., Maurer, P., Wagener, P., and Kocks, C. (1999) *J. Biol. Chem. 274*, 33616−33626.
23. Steffen, P., Schafer, D. A., David, V., Gouin, E., Cooper, J. A., and Cossart, P. (2000) *Cell Motil. Cytoskeleton 45*, 58−66.
24. Xian, W., and Janmey, P. A. (2002) *J. Mol. Biol. 322*, 755−771.
25. Raghunathan, V., Mowery, P., Rozycki, M., Lindberg, U., and Schutt, C. (1992) *FEBS Lett. 297*, 46−50.
26. Rohatgi, R., Ho, H. Y., and Kirschner, M. W. (2000) *J. Cell Biol. 150*, 1299−1310.
27. Fabiato, A., and Fabiato, F. (1979) *Nature 281*, 146−148.
28. Periasamy, A., and Day, R. N. (1999) *Methods Cell Biol. 58*, 293−314.
29. Day, R. N., Periasamy, A., and Schaufele, F. (2001) *Methods 25*, 4−18.
30. Pollok, B. A., and Heim, R. (1999) *Trends Cell Biol. 9*, 57−60.

31. Miyawaki, A., Llopis, J., Heim, R., McCaffery, J. M., Adams, J. A., Ikura, M., and Tsien, R. Y. (1997) *Nature 388*, 882−887.
32. Sato, M., Ozawa, T., Inukai, K., Asano, T., and Umezawa, Y. (2002) *Nat. Biotechnol. 20*, 287−294.
33. Ting, A. Y., Kain, K. H., Klemke, R. L., and Tsien, R. Y. (2001) *Proc. Natl. Acad. Sci. U.S.A. 98*, 15003−15008.
34. Honda, A., Adams, S. R., Sawyer, C. L., Lev-Ram, V., Tsien, R. Y., and Dostmann, W. R. (2001) *Proc. Natl. Acad. Sci. U.S.A. 98*, 2437−2442.
35. Nagai, Y., Miyazaki, M., Aoki, R., Zama, T., Inouye, S., Hirose, K., Iino, M., and Hagiwara, M. (2000) *Nat. Biotechnol. 18*, 313−316.
36. Kurokawa, K., Mochizuki, N., Ohba, Y., Mizuno, H., Miyawaki, A., and Matsuda, M. (2001) *J. Biol. Chem. 276*, 31305−31310.
37. Arai, R., Ueda, H., Kitayama, A., Kamiya, N., and Nagamune, T. (2001) *Protein Eng. 14*, 529−532.
38. Augert, G., Blackmore, P. F., and Exton, J. H. (1989) *J. Biol. Chem. 264*, 2574−2580.
39. Wachter, R. M., Yarbrough, D., Kallio, K., and Remington, S. J. (2000) *J. Mol. Biol. 301*, 157−171.
40. Griesbeck, O., Baird, G. S., Campbell, R. E., Zacharias, D. A., and Tsien, R. Y. (2001) *J. Biol. Chem. 276*, 29188−29194.
41. Kavran, J. M., Klein, D. E., Lee, A., Falasca, M., Isakoff, S. J., Skolnik, E. Y., and Lemmon, M. A. (1998) *J. Biol. Chem. 273*, 30497−30508.
42. Auger, K. R., Serunian, L. A., Soltoff, S. P., Libby, P., and Cantley, L. C. (1989) *Cell 57*, 167−175.
43. Chung, C. Y., Funamoto, S., and Firtel, R. A. (2001) *Trends Biochem. Sci. 26*, 557−566.
44. Katso, R., Okkenhaug, K., Ahmadi, K., White, S., Timms, J., and Waterfield, M. D. (2001) *Annu. Rev. Cell Dev. Biol. 17*, 615−675.
45. Datta, S. R., Brunet, A., and Greenberg, M. E. (1999) *Genes Dev. 13*, 2905−2927.
46. Xia, Z., and Liu, Y. (2001) *Biophys. J. 81*, 2395−2402.
47. Xian, W., Vegners, R., Janmey, P. A., and Braunlin, W. H. (1995) *Biophys. J. 69*, 2695−2702.
48. Srinivasan, S., Wang, F., Glavas, S., Ott, A., Hofmann, F., Aktories, K., Kalman, D., and Bourne, H. R. (2003) *J. Cell Biol. 160*, 375−385.
49. Servant, G., Weiner, O. D., Herzmark, P., Balla, T., Sedat, J. W., and Bourne, H. R. (2000) *Science 287*, 1037−1040.
50. Van Rheenen, J., and Jalink, K. (2002) *Mol. Biol. Cell 13*, 3257−3267.
51. Wymann, M., and Arcaro, A. (1994) *Biochem. J. 298* (Part 3), 517−520.
52. Tolias, K. F., Hartwig, J. H., Ishihara, H., Shibasaki, Y., Cantley, L. C., and Carpenter, C. L. (2000) *Curr. Biol. 10*, 153−156.
53. Janmey, P. A., and Stossel, T. P. (1989) *J. Biol. Chem. 264*, 4825−4831.
54. Varnai, P., Lin, X., Lee, S. B., Tuymetova, G., Bondeva, T., Spat, A., Rhee, S. G., Hajnoczky, G., and Balla, T. (2002) *J. Biol. Chem. 277*, 27412−27422.
55. Matsuda, M., Paterson, H. F., Rodriguez, R., Fensome, A. C., Ellis, M. V., Swann, K., and Katan, M. (2001) *J. Cell Biol. 153*, 599−612.
56. Tran, D., Gascard, P., Berthon, B., Fukami, K., Takenawa, T., Giraud, F., and Claret, M. (1993) *Cell. Signalling 5*, 565−581.
57. Sato, M., Ueda, Y., Takagi, T., and Umezawa, Y. (2003) *Nat. Cell Biol. 5*, 1016−1022.
58. Violin, J. D., Zhang, J., Tsien, R. Y., and Newton, A. C. (2003) *J. Cell Biol. 161*, 899−909.

BI035480W